Vol. 14 (2026): Proceedings of the 2nd International Conference on Artificial Intelligence, Modern Engineering and Environmental Sustainability (IC-AIMEES 2026)
E-ISSN: 3105-0522 P-ISSN：3105-0514
DOI: https://doi.org/10.70267/ ic-aimees.202602183203

Digital Vitality, Finite Energy: A Continuous-Time Framework for Battery Discharge Behavior

Heguang Luan[1], Guangning Wang[2], Yuxuan Lu[1] and Tianrui Chen[3]*

[1]*School of Information Science and Engineering, Harbin Institute of Technology (Wei-hai), Weihai 264209, China*

[2]*School of Computer Science and Technology, Harbin Institute of Technology (Weihai), Weihai 264209, China*

[3]*School of Science, Harbin Institute of Technology (Weihai), Weihai 264209, China*

**Corresponding author: Tianrui Chen.*

Abstract

With the widespread adoption of smartphones, battery endurance has become a critical factor affecting user experience. To systematically characterize battery discharge behavior under real-world usage conditions, this study proposes a Continuous-Time Battery Discharge (CTBD) model. The model is grounded in fundamental physical principles and is progressively extended to incorporate multiple influencing factors, including screen display, processor workload, network connectivity, GPS operation, and background activities. Furthermore, a State of Health (SOH) correction factor is introduced to capture the effects of environmental temperature and battery aging on the effective capacity. Distinct modeling strategies are employed for high- and low-temperature operating conditions. To improve parameter estimation accuracy, a Bayesian inference framework is adopted, combined with the Limited-memory Broyden–Fletcher–Goldfarb–Shanno algorithm with bound constraints (L-BFGS-B) and Laplace approximation. Experimental results on the test dataset show that the proposed model achieves a mean absolute percentage error (MAPE) of 5.54%, demonstrating strong predictive performance. To simulate stochastic signals in practical electronic systems, a random process simulation method based on time discretization, Gaussian sequence generation, and rectangular approximation is developed. Based on this approach, three representative usage scenarios—daily use, office applications, and gaming—are constructed. Under fully charged conditions, the predicted battery lifetimes are approximately 7.8 hours, 5.3 hours, and 4.5 hours, respectively, showing good consistency. Finally, sensitivity analysis is conducted to identify the key factors contributing to battery consumption. The results indicate that screen power consumption dominates (approximately 40%–60%), followed by CPU usage. Based on these findings, the model is further extended to other portable electronic devices, and practical recommendations are proposed from both user behavior and operating system optimization perspectives.

Keywords

CTBD model, bayesian inference, L-BFGS-B, laplace approximation, random process simulation

1. Introduction

1.1 Problem Background

Smartphones have become indispensable tools in both professional and personal life. With technological advancements, users now demand increasingly sophisticated functionality and higher quality from their devices. When purchasing or selecting a smartphone, consumers primarily base their decisions on the trade-off between features and cost. Beyond prioritizing core performance metrics—such as processing chips, memory capacity, display quality (including resolution, refresh rate, and brightness), and camera capabilities—battery endurance is also a critical consideration. Lithium-ion batteries are widely acknowledged as the rechargeable power sources offering the best overall performance [1]. It has been observed that the actual "endurance performance" of a smartphone is not static; even when starting with identical initial charge levels (e.g., fully charged), the usable duration can vary significantly across different usage scenarios—sometimes lasting a full day, while at other times depleting rapidly. The battery life of a smartphone is intrinsically linked to its energy consumption process: the faster the battery discharges, the shorter the endurance, and vice versa.

The energy consumption of a mobile phone battery is determined by a confluence of hardware and software factors—most notably screen activation duration and background application workload—alongside communication modalities, which are contingent upon the wireless network technology and cellular network type in use [2]. These variables directly modulate the device's power draw, thereby impacting the rate of battery depletion. Beyond usage patterns and energy consumption profiles, the perceived battery life is also tightly correlated with the battery's effective capacity. However, battery performance is prone to degradation due to factors such as ambient temperature variations and the number of charge-discharge cycles, which collectively drive the gradual reduction of effective capacity over time [3,4]. This performance deterioration can be quantified by the battery's State of Health (SOH), a key metric that further governs the overall endurance of the mobile device.

Against the backdrop of the ubiquitous adoption of lithium-ion batteries in mobile devices, a systematic dissection of the energy consumption mechanisms of mobile phone batteries and the core determinants governing their effective capacity can facilitate users in optimizing usage behaviors to attain a more stable battery life experience. It also supports the identification and mitigation of external stressors detrimental to battery health, thereby enabling rational battery protection and lifespan extension. Accordingly, this study endeavors to develop a quantitative model for analyzing the power consumption characteristics of mobile phone batteries under diverse usage scenarios, while integrating environmental variables and battery aging factors to evaluate the battery's effective capacity and endurance performance.

1.2 Restatement of the Problem

In light of the aforementioned background and real-world mobile phone usage patterns, we have developed a corresponding mathematical model. This model is designed to estimate the discharge duration of mobile phones under various scenarios by simulating the relationship between State of Charge (SOC) and time across different environmental conditions, thereby addressing the following issues:

- **Problem 1**: Construct a continuous-time mathematical model of battery charge dynamics based on a fundamental characterization of battery power consumption.
- **Problem 2**: Within the established mathematical framework, analyze the impact of screen-on time, processor load, network connectivity, GPS usage, and other background tasks on battery power depletion.
- **Problem 3**: Examine the effects of temperature variations and user-specific power consumption patterns on the battery's effective capacity, and integrate these effects into the mobile phone power consumption model.
- **Problem 4**: Using the developed model, estimate the battery discharge time under different initial charge levels and operating conditions.
- **Problem 5**: Compare the model's predicted results with empirical data to quantify model uncertainty.

- **Problem 6**: Interpret the causes of differential battery power depletion durations and identify the specific contributing factors leading to battery exhaustion in each scenario.
- **Problem 7**: Determine which activities or conditions have the most significant impact on mobile device battery life.
- **Problem 8**: Investigate which activities or conditions have negligible effects on the overall battery endurance of mobile devices.

1.3 Our Work

Figure 1 illustrates the overall research framework of this study, which consists of five main components: the construction of the Continuous-Time Battery Discharge (CTBD) model, parameter estimation, sensitivity analysis, Time-to-Empty prediction, and recommendations:

Figure 1: Overview of our work

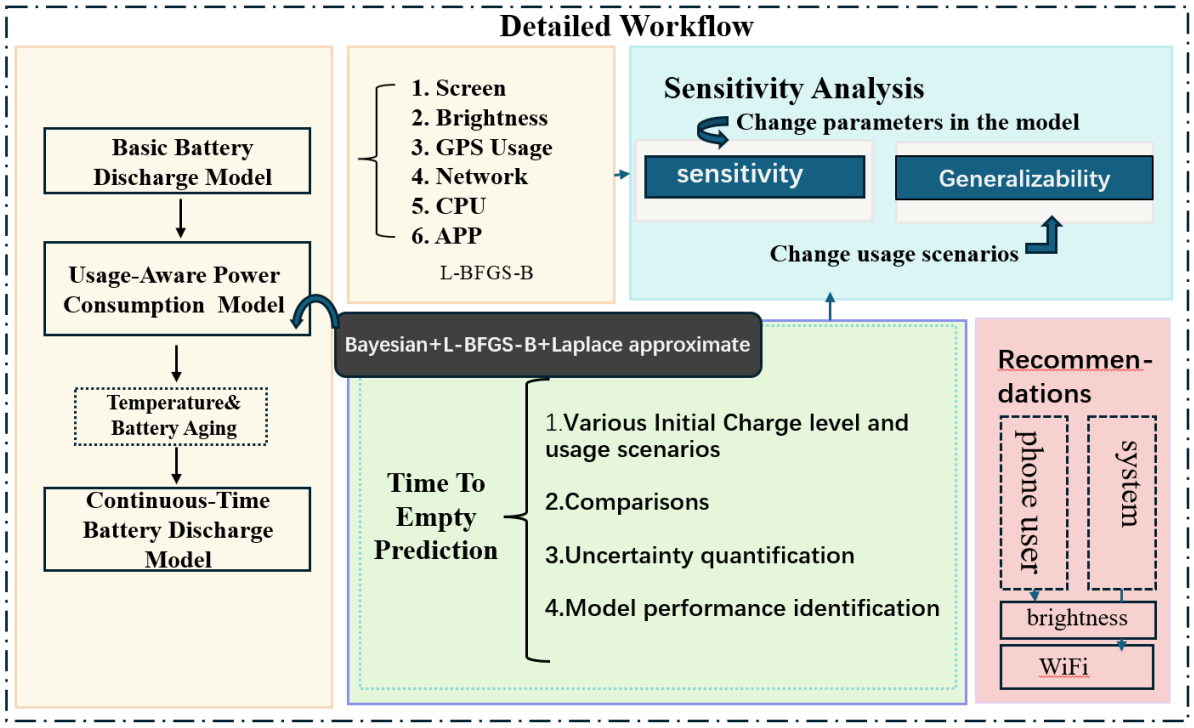

2. Model Preparations

2.1 Assumptions and Justifications

Through an analysis of the issue, the following reasonable assumptions were made to simplify the model:

Assumption 1: The influence of self-discharge of lithium-ion batteries on the power depletion of mobile phone batteries is neglected.

Justification: As documented in the literature [5], the monthly self-discharge rate of lithium-ion batteries is merely 2%–3%. The battery consumption analyzed in this study is thus defined as the time interval from a fully charged state to the next recharge under nominal usage conditions. Considering that the typical charging cycle of smartphones is daily rather than monthly, the self-discharge effect of lithium-ion batteries can be deemed negligible over such short-term periods.

Assumption 2: During the battery discharge process of the mobile phone, no charging behavior occurs, and the operating voltage of the battery remains approximately constant at its nominal value of 3.7 V.

Justification: While the operating voltage of lithium-ion batteries varies with the state of discharge (SOC), it typically remains within a narrow range around the nominal voltage of 3.7 V under typical smartphone usage scenarios [6]. Relative to the impact of system load and usage patterns on power consumption, such voltage fluctuations exert a negligible influence on the overall battery endurance.

Assumption 3: Under short-term operation and nominal working conditions, the coulombic efficiency of the battery approaches unity.

Justification: Under moderate temperature and load conditions, the coulombic efficiency of contemporary lithium-ion batteries typically approaches 100%, with deviations exerting negligible influence on short-term state-of-charge variations.

2.2 Notations

The key mathematical notations used in this paper are listed in Table 1.

Table 1: Notations used in this paper

Symbol	Description	Unit
t	Time variable	hour
$\mathrm{SOC}(t)$	State of charge at time t	\
$Q_{remain}(t)$	Remaining battery capacity at time t	C
Q_{rated}	Rated capacity of the battery	C
$I(t)$	Battery discharge current at time t	mA
C_N	Rated capacity of the battery	mAh
C_M	Effective capacity of the battery	mAh
$P_{total}(t)$	Power consumption at time t	mW
P_{base}	Base power consumption	mW
$P_{screen}(t)$	Power consumption of screen at time t	mW
$P_{cpu}(t)$	Power consumption of CPU at time t	mW
$P_{net}(t)$	Power consumption of network module (WiFi/Cellular) at time t	mW
$P_{GPS}(t)$	Power consumption of GPS module at time t	mW
$P_{app}(t)$	Power consumption of background applications at time t	mW
$SOH(M,T)$	State of health	\
M	Battery cycle number	\
T	Ambient temperature	K

2.3 Data Collection

Since the problem statement does not provide specific datasets, we adopt a **proxy-data-driven method**. Through analysis, we find that smartphone battery consumption is mainly affected by screen usage time, background app activity, GPS usage and ambient temperature.

The principal data sources utilized for model validation are presented in Table 2.

Table 2: Main Data Sources and References

Data Description	Data Source
Users' daily use of mobile phones	https://www.kaggle.com/datasets/vishardmehta/smartphone-battery-health-prediction-dataset
State of Health (SOH) of the Battery	
Cycle Life of Batteries	
Battery Capacity at Low Temperatures	https://m.juda.cn/news/236284.html https://wap.zol.com.cn/ask/x_14767565.html

Due to the privacy-sensitive nature and limited accessibility of fine-grained smartphone battery data, direct real-world measurements are difficult to obtain. Therefore, we construct representative datasets by integrating information from multiple publicly available sources. These include laboratory-reported battery

characteristics, open-source datasets from platforms such as Kaggle, and aggregated performance test results reported by technology reviewers for typical smartphone models.

The collected data are used to determine reasonable parameter ranges and to support scenario-based simulations, rather than to fit a specific device. This approach ensures the generality and robustness of the proposed model.

3. Continuous-Time Battery Discharge Model

3.1 Basic Battery Discharge Model

Ignoring external conditions and focusing solely on battery usage, the state of charge (SOC) at time t can be defined as the ratio of the remaining charge to the rated capacity of the battery:

$$SOC(t)=\frac{Q_{remain}(t)}{Q_{rated}} \tag{1}$$

Under engineering convention, the discharge current is defined as positive. Considering the decrease of stored charge during battery discharge, the charge dynamics can be expressed as:

$$\frac{dQ(t)}{dt}=-\eta I(t) \tag{2}$$

where $I(t)$ denotes the charging/discharging current, and η represents the Coulombic efficiency introduced to account for side reactions and circuit losses. As stated in the assumptions above, we assume $\eta \approx 1$ for simplicity.

By combining (1) and (2), the fundamental relationship describing the evolution of SOC with respect to time can be obtained as:

$$\frac{dSOC(t)}{dt}=-\frac{I(t)}{Q_{rated}} \tag{3}$$

When the time scale is converted from an instantaneous time unit to hours, the rated capacity Q_{rated} can be represented by the nominal battery capacity C_N (Ah), and equation (3) could be stated as:

$$\frac{dSOC(t)}{dt}=-\frac{I(t)}{C_N} \tag{4}$$

According to the relationship between power, current, and voltage $P(t)=U(t)I(t)$ and under the assumptions stated previously, the battery voltage is treated as a constant nominal value U =3.7 V. Substituting this relation into equation (4), we obtain

$$\frac{dSOC(t)}{dt}=-\frac{P(t)}{U(t)\cdot C_N}=-\frac{P(t)}{3.7C_N} \tag{5}$$

This basic discharge model provides a first-order approximation of SOC dynamics and serves as the foundation for subsequent refined models incorporating additional factors such as workload characteristics and temperature variations.

3.2 Usage-Aware Power Consumption Model

The battery consumption of a mobile device is influenced by various factors, including screen brightness, CPU utilization, network connectivity, GPS usage, background application activity, and baseline power consumption [2,7,8]. This paper collectively refers to these parameters as user-behavior-related factors. Given the independence among these variables, the total battery power consumption can be approximately expressed as a linear superposition of the power consumed by each individual module:

$$P_{total}(t) = P_{screen}(t) + P_{cpu}(t) + P_{net}(t) + P_{GPS}(t) + P_{app}(t) + P_{base} \tag{6}$$

1) Screen Brightness Power Consumption

Research findings demonstrate a near-linear positive correlation between the power consumption of a smartphone screen and its luminance [8]. In practical usage, screen luminance varies with user interactions and contextual scenarios. Accordingly, we model screen luminance as a time-dependent function with stochastic properties, and express the screen power consumption as follows:

$$P_{screen}(t) = k_{screen} \cdot S \cdot L_{norm}(t) + k_1 \tag{7}$$

In the formula, k_{screen} denotes the proportional coefficient associated with the maximum power consumption per unit screen area and screen utilization; S represents the screen area of the mobile device (unit: cm²); $L_{norm}(t)$ denotes the normalized screen luminance at time t, defined as the ratio of the instantaneous screen luminance to the maximum screen luminance, with the constraint $L_{norm}(t) \in [0,1]$; and the constant term k_1 refers to the baseline power consumption of the screen (unit: mAh).

2) Impact of GPS Usage on Power Consumption

Studies have shown that GPS positioning time t_{fix} is negatively correlated with signal strength G [9]. In practical operation, the GPS module remains active until positioning is completed; therefore, longer positioning durations lead to increased energy consumption. It can thus be inferred that the power consumption of the GPS module in mobile devices is positively correlated with its operating duration. The relationships among positioning time t_{fix}, signal strength G, and GPS power consumption P_{GPS} are illustrated in Figure 2.

Figure 2: Relationship between P_{GPS} and Operating time

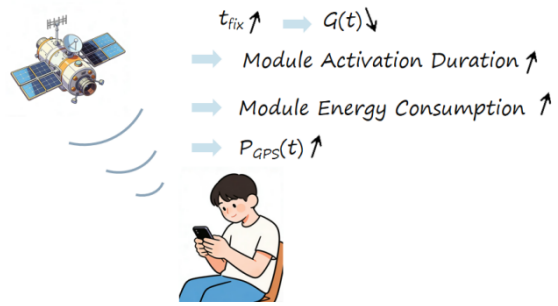

In practical applications, the GPS module operates continuously until a location fix is acquired. Accordingly, extended positioning durations lead to elevated energy consumption. It can thus be inferred that the power consumption of the GPS module in mobile devices exhibits a positive correlation with the positioning time.

Based on the above analysis, we have constructed a relational model between the power consumption of the GPS module and signal strength:

$$P_{GPS}(t) = k_{gps} \frac{1}{G_{norm}(t)} + k_2 \tag{8}$$

In the formula, k_{gps} denotes the proportionality coefficient, $G_{norm} \in [0,1]$ represents the normalized signal strength, and the constant term, k_2 refers to the baseline power consumption of the GPS module (unit: mAh).

3) Network Communication Power Consumption

Research demonstrates that the power consumption of the network module during active connectivity is positively correlated with the data transmission rate [7], which is expressed as follows:

$$P_{net}(t) = c\alpha R(t) + k_3 \tag{9}$$

$$\alpha = \begin{cases} 1 & \text{WiFi} \\ 1.16 & \text{4G} \\ 1.33 & \text{5G} \end{cases} \tag{10}$$

Using the data transmission rate under WiFi connectivity as a benchmark and referencing data from technical reviewers, c denotes the proportionality coefficient, α represents the multiplicative factor for module power consumption across different network connection modes, and the constant term k_3 refers to the baseline power consumption of the network module.

4) CPU Utilization Power Consumption

The power consumption of the mobile device CPU module exhibits a quadratic correlation with CPU utilization [10]. The model is constructed as follows:

$$P_{cpu}(t) = a\rho(t)^2 + b\rho(t) + k_4 \tag{11}$$

In the formula, $\rho(t)$ denotes CPU utilization, a and b represent proportional coefficients, and k_4 refers to the baseline power consumption of the CPU module.

5) Background Application Activity Power Consumption

Analogous to Scenario (1), In practice, the number of background applications fluctuates in response to user operations and varying usage scenarios. Given the difficulty in precisely quantifying this dynamic process, the present study conceptualizes the number of background applications as an indeterminate function of time t, denoted as $N(t)$. Accordingly, the power consumption of background applications in mobile devices is defined as follows:

$$P_{app}(t) = P_{avg}N(t) + k_5 \tag{12}$$

In light of the complexity of application power consumption, the average power consumption of the application is designated as P_{avg}, where k_5 denotes the baseline power consumption of the application module.

6) Baseline Power Consumption of Mobile Device

Based on equations (1) to (5), it can be observed that each functional module consumes a load-independent baseline power during operation. This paper integrates the baseline power consumption of all functional modules with the intrinsic baseline power consumption of the mobile device, collectively defining them as the static power consumption P_0. Equation (6) can thus be re-expressed as follows:

$$P_{total}(t) = P_{screen}(t) + P_{GPS}(t) + P_{net}(t) + P_{cpu}(t) + P_{app}(t) + P_0 \tag{13}$$

Accordingly, the CTBD model is derived as follows:

$$\frac{dSOC(t)}{dt} = -\frac{P_{total}(t)}{3.7C_N} \tag{14}$$

3.3 Model Refinement

Variations in historical usage patterns lead to differences in the effective capacity of batteries. Thus, even for the same smartphone, identical power-consuming operations performed under different historical usage conditions will inevitably result in different battery depletion rates due to variations in the battery's intrinsic effective capacity. Additionally, temperature is a key factor affecting the battery discharge rate in practical scenarios [4,11]. Incorporating these two factors, we first establish a baseline model under ideal conditions and then introduce correction factors to refine the basic model. The effects of temperature and historical usage on the actual effective capacity of the battery are illustrated in Figure 3.

Figure 3: Effects of Temperature and Historical Usage on Battery Capacity

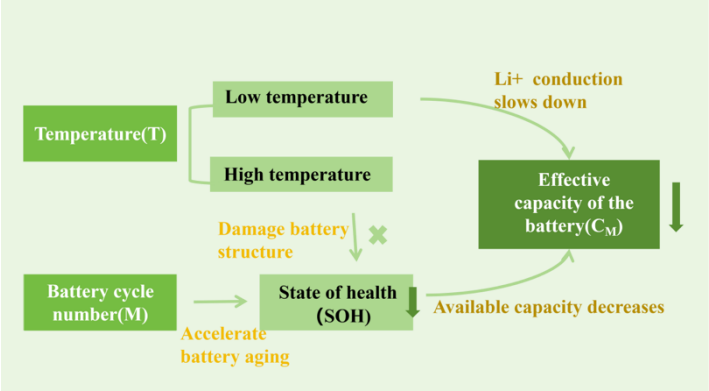

3.3.1 Battery Aging and Usage Habit Effects

Studies have shown that continuous charge-discharge cycling triggers irreversible electrochemical reactions in lithium-ion batteries, causing degradation of electrode materials and subsequent capacity fade [10]. Consequently, lithium-ion batteries are typically designed with a limited cycle life, beyond which their functional performance is significantly impaired. The ambient operating temperature of a mobile device significantly affects its battery endurance. Specifically, compared to normal temperatures, high-temperature conditions accelerate electrochemical reactions within the battery, driving rapid structural changes in lithium-ion cells and causing irreversible damage that leads to battery degradation [4]. Prolonged exposure to elevated temperatures will inevitably reduce the battery's effective capacity and impair its state of health (SOH) [11]. Yu et al. [12] further demonstrated that the state of health (SOH = current remaining capacity / nominal capacity) of batteries exhibits a significant correlation with temperature. Incorporating these factors, we introduce a battery lifespan model that uses cycle count as an indicator of historical usage—where one full charge–discharge process constitutes a single cycle. Prolonged usage of mobile devices increases battery cycle counts, which in turn leads to reduced battery lifespan and decreased effective capacity.

Given that each charge–discharge cycle impacts the internal electrochemical state of the battery and follows a nonlinear trend [12,13], we adopt the formula proposed by Yu et al. [11], as follows:

$$SOH(M,T) = 1 - \beta \exp\left(\frac{-E_a}{\text{Rug} \cdot T}\right) \cdot M^n \tag{15}$$

In the equation: n represents the time-dependent enhancement factor; β denotes the cycle count influence coefficient, which indicates the impact of the number of cycles on battery capacity; M stands for the cycle count; T is the ambient temperature (unit: K); E_a refers to the activation energy (unit: KJ/mol); Rug represents the universal gas constant, commonly taken as 8.314 J/(mol·K).

This formula can clearly characterize the inherent relationship that the longer the service time of the mobile phone, the more the charging cycles, the lower the battery's available capacity, and the poorer the battery health state; such a characterization of battery health can also reflect the practical phenomenon that high temperatures accelerate lithium-ion battery aging.

3.3.2 Low Temperature Effects

The discharge of lithium-ion batteries is essentially an ion exchange process occurring in the electrolyte solution. At low temperatures, the migration rate of ions decreases, which in turn reduces the battery's discharge rate and discharge capability—namely, its available capacity [14]; the lower the temperature, the more pronounced the capacity reduction. This process is nevertheless reversible: the available capacity of the battery will recover once the ambient temperature returns to the normal range.

At the ambient temperature T_{best}, all performance metrics of the mobile phone battery reach their optimal levels. Taking this temperature as the critical threshold, the battery's effective capacity exhibits a more pronounced decline as the actual temperature deviates further from T_{best}, with the effective capacity remaining strictly greater than zero at all times. In this paper, a proportional coefficient for the battery's state

of health ($\mathrm{SOH} \cdot C_N$) and available capacity γ is introduced. Temperatures below T_{best} are uniformly defined as low-temperature conditions, for which the coefficient *r* in the high-temperature model is set to 1; all other temperature conditions are modeled under the high-temperature framework. Based on the above definitions, a Gaussian decay function is employed to characterize the influence of low-temperature conditions on the battery's effective capacity:

$$\gamma(T) = \exp(-\alpha_2 (T_i - T_{best})^2), T_i <= T_{best} \tag{16}$$

In this formula: γ denotes the proportional coefficient of the battery's available capacity under the current state of health (SOH); T_i denotes the ambient temperature (unit: K).

By integrating Equations (14), (15), and (16), we ultimately derive the Cycle-Temperature Battery Degradation (CTBD) model.

$$\begin{cases} \dfrac{dSOC(t)}{dt} = -\dfrac{P_{tatal}(t)}{3.7 \cdot C_N \cdot SOH(M,T)\gamma(T)} \\ SOC(0) = SOC_0 (\text{State of Charge under Initial Conditions}) \end{cases} \tag{17}$$

4. Parameter Estimation, and Model Validation

4.1 Parameter Estimation of UAPC Model

To estimate the unknown parameters in the battery discharge model, it is necessary to adopt a rational parameter estimation method. Given the nonlinear structure and high-dimensional parameter space of the model, traditional fitting approaches, such as the least squares method, often involve high computational costs and exhibit slow convergence. Therefore, we propose a comprehensive framework based on Bayesian inference [15,16], the L-BFGS-B algorithm (a quasi-Newton method), and Laplace approximation to improve the robustness of parameter estimation.

Based on a large volume of user behavior data, the screen brightness $L(t)$, CPU utilization $\rho(t)$, number of background applications $N(t)$, and data transmission rate $R(t)$ as constants to reflect the macroscopic performance under typical usage scenarios. Under these conditions, the observed value of the total power consumption of the smartphone can be calculated using the following formula:

$$P_i^{obs} = \frac{V_{nor} C_{0,i}}{t_i} \tag{18}$$

All the parameters to be estimated in the model constitute the parameter vector θ. The predicted power consumption for a sample is denoted as $P_i^{pred}(\theta)$, and the residual $r(\theta)$ is defined as:

$$r(\theta) = P_{pred}(\theta) - P_{obs} \tag{19}$$

$$\theta = \left[P_0, k_{screen}, a, b, c, d, e, P_{avg} \right]^{\mathrm{T}} \tag{20}$$

In this formula: $P_{pred}(\theta)$ represents the observed power consumption of the sample.

For each component of the parameter vector θ, assuming their observational errors follow mutually independent normal distributions, the residual $r(\theta)$ should obey a high-dimensional normal distribution. Evidently, since the residuals are correlated with both the predicted and observed power, the likelihood function similarly follows a high-dimensional normal distribution:

$$p(Y|\theta) \propto \exp\left(-\frac{1}{2\sigma^2} \|r(\theta)\|_2^2 \right) \tag{21}$$

Y denotes the observed samples available for parameter estimation.

According to the maximum entropy principle in information theory, the prior distribution of each component of the parameter vector θ is assumed to follow a normal distribution. Furthermore, the parameters are normalized to eliminate the influence of measurement units:

$$\tilde{\theta} = D\left(\theta - \theta_{\min}\right) \tag{22}$$

$$D = diag\left(\frac{1}{\theta_i^{\max} - \theta_i^{\min}}\right) \tag{23}$$

Here D denotes the scaling matrix, and $\tilde{\theta}$ represents the normalized parameter vector. Consequently, the prior probability of the parameter vector is also assumed to follow a multivariate normal distribution:

$$p\left(\theta\right) \propto \exp\left(-\lambda \left\|\tilde{\theta}\right\|_2^2\right) \tag{24}$$

According to Bayesian inference, the posterior probability is given by the product of the prior probability and the likelihood function:

$$p\left(Y|\theta\right) \propto p\left(Y\right) p\left(\theta|Y\right) = \exp\left(-J\left(\theta\right)\right) \tag{25}$$

Clearly, when the empirical probability function attains its maximum value, the corresponding parameter vector θ represents the optimal estimate. Therefore, the problem can be reduced to determining the minimum of $J\left(\theta\right)$:

$$J\left(\theta\right) = \frac{1}{2\sigma^2}\left\|r\left(\theta\right)\right\|_2^2 + \lambda\left\|\tilde{\theta}\right\|_2^2 \tag{26}$$

Given the high-dimensional nature of the parameter space, heuristic algorithms such as the Genetic Algorithm (GA) and Simulated Annealing (SA) can be employed to perform global search for the aforementioned minimization problem. However, in this study, the more efficient Limited-memory Broyden–Fletcher–Goldfarb–Shanno algorithm with bound constraints (L-BFGS-B) is adopted. This algorithm is based on the quasi-Newton method, and Egidio et al. further extended the classical BFGS algorithm to enable optimization under limited-memory conditions with bound constraints [17]. As a result, it serves as an effective approach for solving high-dimensional optimization problems. The main steps of the algorithm are as follows:

Step 1: Randomly select K initial values within the solution space of the parameter vector, and initialize the global minimum value and the globally optimal parameter vector.

Step 2: For each initial value, compute the gradient $\nabla_\theta J\left(\theta\right)$ and construct the projection vector. A global search is then performed along the negative direction of the projected gradient. The iteration continues until the maximum number of iterations or the specified tolerance is reached.

Step 3: Traverse the next randomly generated initial value and repeat the previous step. After the iteration terminates, compare the obtained result with the current global minimum and update the optimal parameter vector accordingly.

The L-BFGS-B algorithm is capable of exploring the entire parameter space and conducting searches along the gradient direction, offering the advantage of fast convergence. The parameter vector produced by this algorithm can therefore be taken as the estimated parameter values.

Since various sources of uncertainty exist in the parameter estimation process, these uncertainties need to be quantified. Alexander Immer et al. (2021) proposed a Laplace approximation method that linearizes the network parameters at the maximum a posteriori estimate [18]. Let the significance level α be set to 0.05. The 95% confidence interval can then be estimated using the Laplace approximation:

Step 1: Determine the mode of the probability distribution, denoted by $\hat{\theta}$, which corresponds to the output obtained from the aforementioned L-BFGS-B algorithm.

Step 2: Perform a second-order Taylor expansion at the point $\hat{\theta}$ to obtain an approximate probability distribution around the point $\hat{\theta}$, denoted as $N\left(\hat{\theta}, H^{-1}\right)$.

Step 3: Compute the 95% confidence interval of the parameters:

$$\theta_j \approx \hat{\theta}_j \pm 1.96\sqrt{\Sigma_{jj}} \tag{27}$$

Where, w represents the covariance matrix.

The results of the parameter estimation are presented in Table 3

Table 3: The Result of Parameter Estimation of UAPC model

Parameter	Mean	2.5% Lower	97.5% Upper
P_0	260.821	251.132	271.996
k_{screen}	0.117	0.116	0.118
a	523.420	500.710	585.380
b	155.312	148.890	164.190
c	5.590	4.470	6.356
P_{avg}	2.458	2.870	2.870

4.2 Parameter Estimation for Correction Factors

(1) For the low-temperature correction factor, we calculated its value based on the experimental test data [19] obtained under both low-temperature conditions as follows:

Under the first condition: $\alpha_2 \approx 5.44 \times 10^{-4}$

Under the second condition: $\alpha_2 \approx 5.06 \times 10^{-4}$

Given the minimal discrepancy between the two calculated values, their average was computed to determine the parameter $\alpha_2 = 5.25 \times 10^{-4}$.

(2) The model parameters related to life expectancy were estimated via the least squares method for curve fitting, and the fitting results are presented in Table 4.

Table 4: Estimated Parameters of the Aging Correction Model

Parameter	**Explanation**	**Estimated Value**	**Unit**
β	Aging correction coefficient	0.98	-
E_a	Activation energy	9.43	kJ/mol
n	Degradation exponent	0.4237	-

4.3 Model Validation

Upon completing the parameter estimation for base power consumption, CPU modules, screen, and network power usage, a validation analysis of the model's effectiveness is conducted to verify the fitting accuracy and practical applicability of the developed overall battery power consumption model. The model's performance is evaluated across multiple dimensions: overall prediction efficacy, reasonableness of module decomposition, and error characteristics. The fitting of Time-to-Empty and SOH is shown in Figure 4.

Figure 4: Time-to-Empty Fitting and SOH Fitting (Predicted vs. Actual)

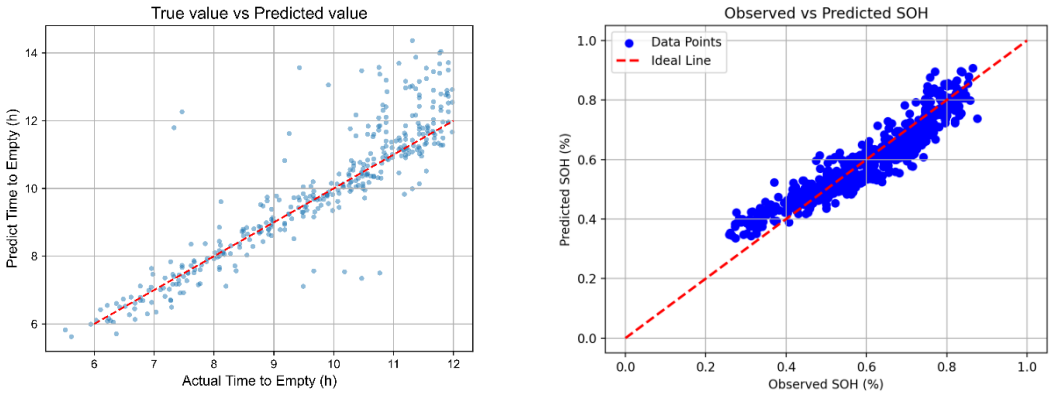

5. Time-to-Empty Predictions for Different Situations

5.1 Discrete-Time Stochastic Signal Simulation Based on Gaussian Noise

Within parameter estimation frameworks based on large-scale datasets, it is common practice to treat screen brightness $L(t)$, CPU utilization $\rho(t)$, and data transmission rate $R(t)$ as fixed values to capture the statistical characteristics of macroscopic user behavior. However, in actual hardware systems, the instantaneous values of these physical quantities are often subject to circuit noise, scheduling fluctuations, and channel interference—exhibiting stochastic time-varying properties. To address this issue, we draw on the work of Jing Pan et al., who investigated chaotic signals from the perspective of stochastic processes [20]. Based on the modeling analysis of low-frequency and high-frequency noise in circuits by Deen, M. J. et al. [21], we model $L(t)$, $\rho(t)$, and $R(t)$ as sequences of random variables perturbed by white Gaussian noise. Taking $L(t)$ as an example, the model can be expressed as:

$$L(t) = \bar{L} + \varepsilon(t) \tag{28}$$

$$\varepsilon(t_i) \sim N(0, \sigma^2), i = 1, 2, 3..., n$$

This study proposes a numerical simulation methodology termed 'Time Discretization – Gaussian Sequence Generation – Rectangular Approximation' to reasonably approximate actual noise environments. The detailed procedure is schematically outlined in Figure 5 as follows:

Step 1: Temporal Discretization. Within the observation interval $[0, T]$, a discrete time step T_0 is selected to uniformly partition the continuous time axis into N subintervals.

Step 2: Gaussian Sequence Generation. For each type of physical quantity, a random value conforming to a specified Gaussian distribution is sampled at the start of every subinterval. Sampling instants are mutually independent—reflecting the short-term uncorrelated nature of noise, which aligns with the common assumption of white Gaussian noise in electronic systems.

Step 3: Rectangular Approximation. Within each subinterval, the function value is held constant at the initial sampled value, forming a piecewise constant approximation. When T_0 is sufficiently small, this approximation effectively simulates a continuous stochastic process.

Figure 5 illustrates the procedure of random process simulation in the form of a function graph. In various scenarios, by adjusting the means and variances of the Gaussian distributions corresponding to the $L(t)$, $\rho(t)$, and $R(t)$ parameters to quantify uncertainty, and applying the aforementioned simulation methodology, the variability in smartphone battery discharge times under different conditions can be investigated.

Figure 5: Schematic Diagram of Stochastic Analysis Procedure Steps

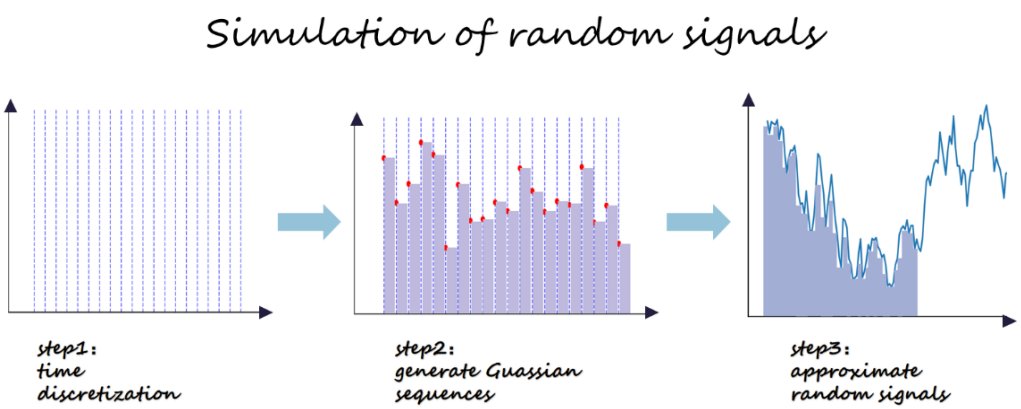

5.2 Time-to-Empty Time Predictions for Different Usage Scenarios

(1) From the Perspective of User Factors:

Given the complexity of usage scenarios, we selected three typical conditions for predicting battery discharge time: gaming (high load), office tasks (medium load), and daily use (low load). To rigorously evaluate the applicability of our model, device parameters were configured with reference to the iPhone 17 specifications, including a rated battery capacity of 3692 mAh and a screen area of 149.6 × 71.5 mm.

The mean values of the relevant parameters and variables are presented in Table 5.

Simulations of stochastic processes yielded the discharge time profiles for the three scenarios, as illustrated in Figure 6. The data largely align with actual results. The comparison reveals that $t_{Game} < t_{Office} < t_{Daily}$, indicating that the battery's state of charge (SOC) declines most rapidly during gaming sessions. According to the proposed model, the gaming scenario exhibits the highest values of power-related parameters and variables, resulting in the heaviest device load and the shortest battery discharge time, which is consistent with practical observations. Furthermore, based on three representative usage scenarios, the Time-to-Empty is simulated under different initial State of Charge (SOC) conditions, as shown in Figure 7.

Table 5: Mean values of relevant parameters and variables

Scenarios	α	$N(t)$	$\rho(t)$	$L(t)$	$R(t)$
Gaming	1.33	3	0.6	0.6	250
Office	1.16	8	0.3	0.4	200
Daily	1.00	2	0.2	0.2	150

Figure 6: Energy Consumption in Different Scenarios

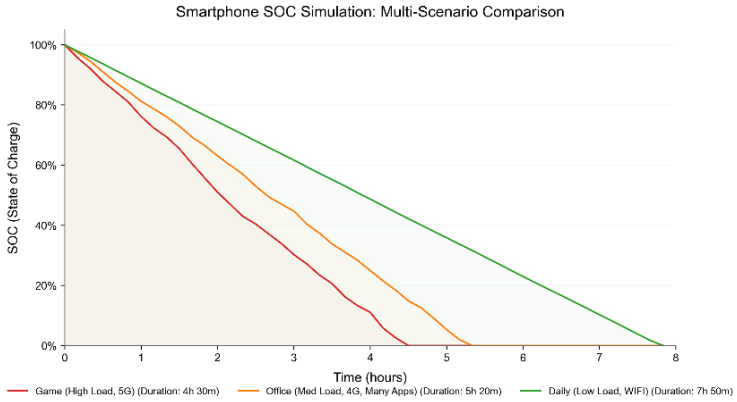

Figure 7: Heatmap of Time-to-Empty Time under Different Conditions

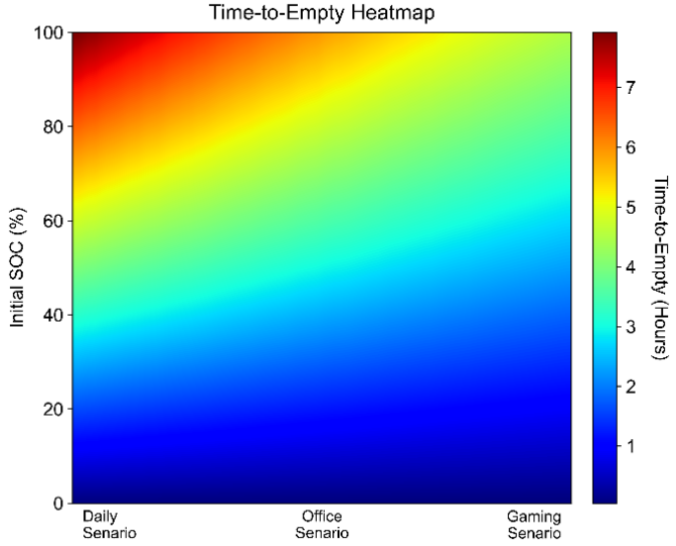

Figure 8: The influence of Temperature and Cycles on Time-to-Empty time

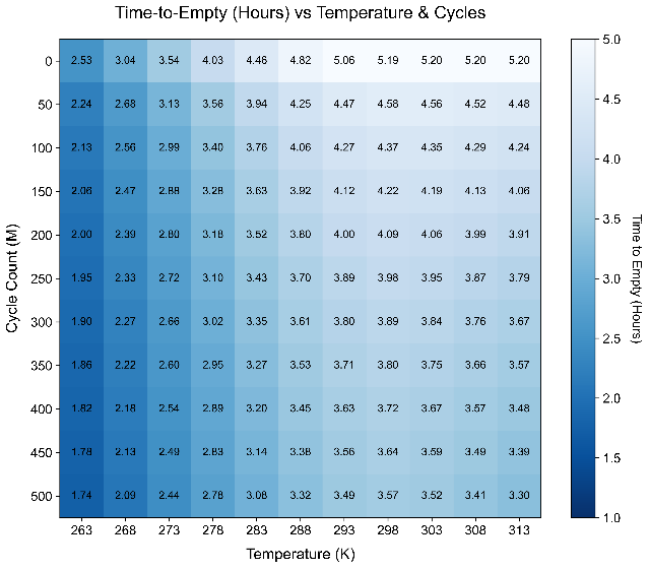

(2) From the State of Health factors:

The above analysis indicates that the effective battery capacity is jointly affected by environmental temperature and battery aging. Accordingly, Figure 8 illustrates the Time-to-Empty under an office usage scenario with a fully charged initial condition, across different temperatures and aging levels, presented as a heatmap.

5.3 Discharge Duration

In our analysis based on three typical scenarios, the discharge time under varying initial SOC (SOC_0) conditions was calculated. The results indicate that, under identical operating conditions, a lower SOC_0 corresponds to a shorter discharge period. This phenomenon is effectively elucidated mathematically by Equation (20)

5.4 Scenario Comparison

Figure 9 illustrates the proportion of power consumption attributed to different functional modules of smartphones under three typical usage scenarios. Through a comparative analysis of power consumption distribution across three typical usage scenarios for mobile phones, we have identified the display as the

dominant factor affecting battery life, accounting for approximately 50% to 60% of the total power consumption. Unexpectedly, the CPU emerged as the second most significant power-consuming component, contributing roughly 20% to 25% across all three scenarios. Notably, high-load conditions did not substantially increase the CPU's share of power consumption. Meanwhile, background applications consistently accounted for a minimal proportion of power usage, exerting negligible impact on overall battery endurance.

Figure 9: Average Power Proportion Contribution Breakdown in Three Scenarios

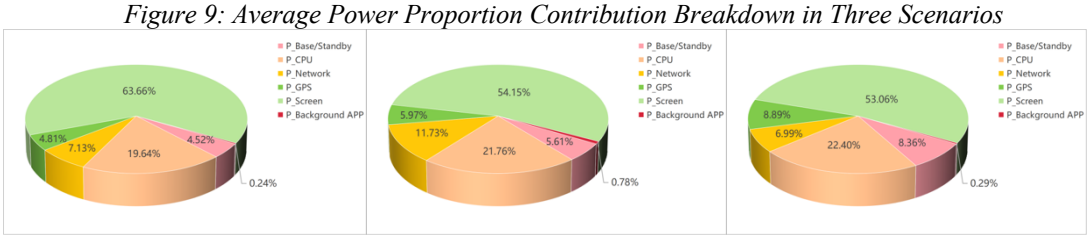

Furthermore, the thermal imaging plot (the one depicting temperature distribution) clearly demonstrates that low-temperature conditions significantly impair smartphone battery endurance. Overall, screen power consumption and low ambient temperature constitute the primary factors affecting battery life.

6. Sensitivity Analysis and Key Factor Identification

6.1 Sensitivity to Usage Patterns and Environmental Conditions

(1) Adjustment of modeling assumptions: In the initial assumptions of the article, we assumed that the Coulomb efficiency of the lithium battery in the mobile phone was approximately 100%. Even considering factors such as the external environment and energy conversion in reality, the Coulomb efficiency could reach 0.8 to 0.95, which had a very small impact on the model's prediction of the time-to-empty.

(2) Sensitivity analysis of parameter values: In the model construction and parameter estimation sections, we assume that the standby power consumption(P_{base}) of the smartphone and the power consumption of the GPS (P_{GPS}) module remain constant. However, considering the inherent electrical noise within the smartphone system and the changes in the external environment, P_{base} and P_{GPS} will also experience random fluctuations. Based on the study by X. Chen et al. on the power consumption of various smartphone components, the following conclusions can be drawn: The typical standby power consumption P_{base} of a smartphone ranges from 50mW to 200mW, and the power consumption of the GPS module ranges from 120mW to 200mW [22]. By changing P_{base} and P_{GPS} while keeping the initial SOC value at 1 and the phone's usage scenario in the office mode, the trend of the idle time t is shown in the Figure 10. Clearly, the time-to-empty changes within a very narrow range with respect to the two factors, meaning that the standby power consumption and the power consumption of the GPS module have a very small impact on the time-to-empty prediction. They have a very low sensitivity to the model, indicating that treating them as constants is a reasonable assumption.

(3) Analysis of the Fluctuation Adjustment of Usage Patterns: In the previous scenario simulations, it was assumed that users maintain a single behavior pattern throughout the continuous battery discharge process. The study by Chen, C. Y. et al. found that smartphone users derive pleasure from complex usage patterns, leading to dependence on their devices [23]. Therefore, in real-world usage, users frequently switch among three typical scenarios: daily use, office work, and gaming. To capture this characteristic, five composite scenarios are constructed by varying the proportion of user behaviors over time, and the resulting State of Charge (SOC) trajectories are simulated, as shown in Figure 11.

The results indicate that variations in scenario proportions have a significant impact on the prediction of Time-to-Empty. In particular, due to the substantial differences in usage patterns between gaming and daily scenarios, fluctuations in their proportions lead to more pronounced effects on the predicted outcomes. Furthermore, these findings demonstrate that the proposed model maintains strong predictive capability under complex and dynamic real-world conditions.

Figure 10: Impact of P_{base} and P_{gps} on Battery Life

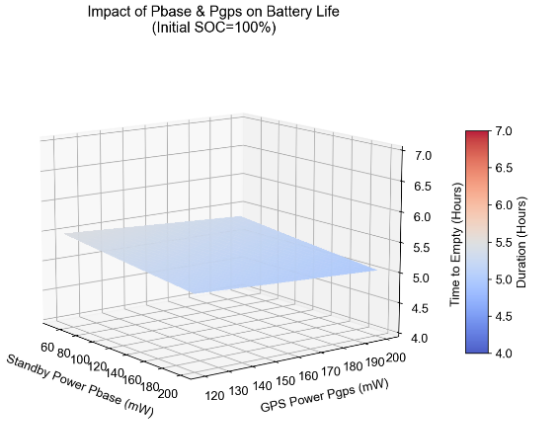

Figure 11: Battery Discharge Profiles by User Scenario Mix

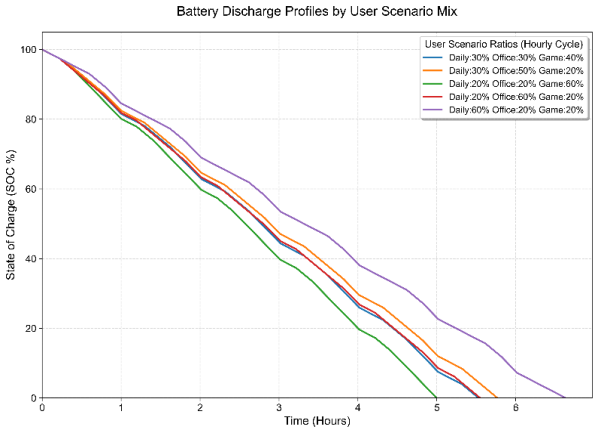

6.2 Key Factor Identification

The CPU in a smartphone can be regarded as the device's central processing unit, responsible for executing the operating system, processing application instructions, and coordinating various hardware components. Consequently, it represents a key factor influencing the overall power consumption of a smartphone.

Based on the mathematical model established in the previous section, under a gaming usage scenario, Figure 12 illustrates the variation in smartphone's time-to-empty with respect to CPU load and the initial battery level. It can be observed that the time-to-empty exhibits noticeable changes, indicating that the CPU module plays a crucial role in the overall power consumption of smartphones. Moreover, these results highlight the importance of improving smartphone energy efficiency through the optimization of CPU performance.

Figure 12: The variation curve of time-to-empty with CPU load

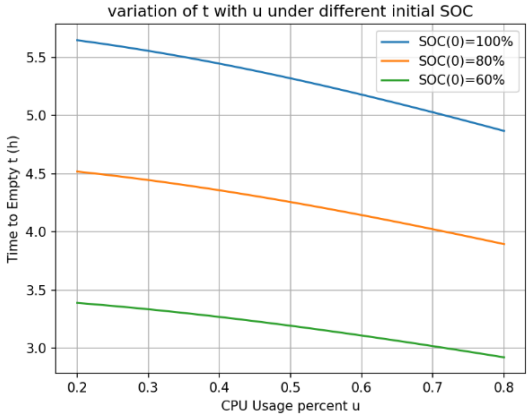

7. Discussion and Recommendations

Based on the aforementioned assumptions and analysis, this section systematically summarizes several practical recommendations for smartphone users and operating system design. Furthermore, the smartphone power consumption model is extended to other portable electronic devices, specifically wireless earphones. Based on this power consumption model, a modeling approach for the power consumption of wireless earphones is proposed, thereby demonstrating the broad applicability of the model.

7.1 Practical Recommendations for Users and Systems

Recommendations for Users: The pie chart of smartphone power consumption indicates that the display module accounts for the vast majority of the total energy consumption. Therefore, users are advised to reduce screen brightness whenever high brightness is unnecessary. Although the power consumption of background applications is relatively small, the accumulated energy usage can become significant if these applications are not cleared over extended periods. In addition, users should remember to disable the GPS function after using navigation or map services. It is also important to note that frequent charging cycles accelerate the aging of lithium-ion batteries. Consequently, users are encouraged to adopt proper charging habits in order to prolong battery lifespan.

Recommendations for Operating System Design: The operating system serves as the core component of smartphone software architecture. A well-designed operating system can often provide significant benefits in terms of energy efficiency. We recommend enabling automatic screen brightness adjustment, optimizing system scheduling by limiting the number of background applications, and automatically connecting to Wi-Fi networks whenever conditions permit. Implementing such effective energy-saving strategies can enhance the overall competitiveness of smartphone products. This recommendation is consistent with the findings of Swapnili P. Karmore et al. on battery monitoring and analysis [24].

7.2 Model Extensions and Limitations

Strengths:

1) The model proposed in this study is developed based on fundamental physical principles and comprehensively incorporates multiple influencing factors, including the display, CPU, network, GPS, and background applications. The mathematical framework is constructed progressively from simple to more complex formulations. In addition, the effects of temperature variations and battery aging on lithium-ion battery performance are also taken into account, enabling the model to predict the remaining battery life of smartphones with reasonable accuracy under most usage scenarios.
2) The parameter estimation in this study is based on nearly 5,000 records of real smartphone usage data from users. By integrating statistical methods with physical principles, the proposed parameter estimation approach demonstrates strong robustness and reliability.
3) Based on the developed model, we further propose a general power consumption modeling method for electronic devices. This method requires only a small number of observable physical variables to accurately predict battery consumption, which provides strong potential for engineering applications. Furthermore, the model is extended to other portable electronic devices, specifically wireless earphones, thereby further validating its general applicability.
4) We innovatively employ techniques such as time discretization, Gaussian sequence random generation, and rectangular approximation of random signals to simulate realistic noise environments in electronic systems. The results indicate that the model maintains strong predictive performance under practical operating conditions.

Weaknesses:

1) The model and related assumptions in this study are primarily based on the average technological level of contemporary smartphones. Since different smartphone brands and models may exhibit variations in both hardware and software performance, the predictive performance of the model may not be optimal in certain specific cases.

2) To simplify the modeling process, this study assumes that different smartphone modules operate independently, thereby neglecting the potential coupling effects that may exist among them.

7.3 Development

As an important category of portable electronic devices, smartphones share significant similarities with other portable devices in terms of structural design and usage patterns. The study by Shuhaizar Daud et al. found that CPU power consumption largely depends on idle time and processor load [25]. As illustrated in Figure 13, the CPU power consumption of electronic devices can generally be expressed as a function of CPU utilization, which provides a theoretical basis for extending the proposed model to other devices.

However, differences in power consumption characteristics and battery types still exist across devices. Therefore, in practical applications, the model should be appropriately adapted to specific device types and usage scenarios, and its parameters should be calibrated according to device-specific characteristics.

Figure 13: Model Extension of Other Electronic Devices

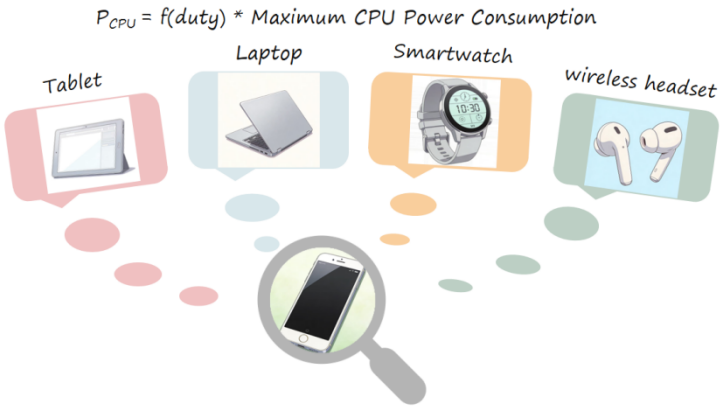

Taking wireless earbuds as an example:

Since wireless earbuds lack a screen and GPS, the power consumption parameters P_{screen} and P_{GPS} are set to zero. Meanwhile, the background power consumption—primarily utilized for maintaining connections and monitoring battery status—represents a stable and minimal value, which can be treated as a constant and included as part of the standby power. Bluetooth power consumption, being the dominant component of network connectivity power usage, is primarily influenced by the data transmission rate. Thus, it is simplified to Bluetooth power consumption, thereby eliminating the impact of the scaling factor α associated with different connection methods. As the CPU in earbuds is predominantly dedicated to audio processing with a fixed core frequency, dynamic power consumption solely depends on the duty cycle of operation. Accordingly, the following equation can be applied as an equation.

The load factor of the mobile phone is related to the mode in which the headphones are operating, such as listening + active noise cancellation (ANC), standby, and listening. At the same time, the battery of the wireless headphones still conforms to the characteristics of the lithium-ion battery of the mobile phone, but the relevant parameters need to be corrected according to the different battery parameters.

By inputting the various data of wireless headphones, the discharge time can be predicted. Similarly, our model is also applicable to other portable devices.

8. Conclusion

This study presents a comprehensive Continuous-Time Battery Discharge (CTBD) model that systematically characterizes smartphone battery behavior under real-world usage conditions. The model successfully quantifies the dominant influence of screen and CPU power consumption, integrates the critical effects of battery aging and ambient temperature through an SOH correction factor, and achieves high predictive accuracy (MAPE 5.54%) using a Bayesian inference framework. Furthermore, a novel stochastic simulation method enables realistic discharge time predictions for varied usage scenarios. Sensitivity

analysis identifies key drivers of rapid depletion, and the findings are extended to propose practical, evidence-based optimization strategies at both the user and operating system levels, offering a scalable framework for improving energy management in portable electronics.

References

[1] FENG, X., YANG, Z., ZHANG, Q., SU, Y., QIAO, Y., LIU, S., ... & WANG, D. (2018). Smart devices battery life technology trends. Science & Technology Review, 36(6), 97-104. (in Chinese)

[2] Pramanik, P. K. D., Sinhababu, N., Mukherjee, B., Padmanaban, S., Maity, A., Upadhyaya, B. K., ... & Choudhury, P. (2019). Power consumption analysis, measurement, management, and issues: A state-of-the-art review of smartphone battery and energy usage. ieee Access, 7, 182113-182172.

[3] Takeno, K., Ichimura, M., Takano, K., & Yamaki, J. (2003, October). Methods of energy conservation and management for commercial Li-ion battery packs of mobile phones. In The 25th International Telecommunications Energy Conference, 2003. INTELEC'03. (pp. 310-316). IEEE.

[4] Hu Z K, Peng P, Sun W Z, et al. Research progress on influence of environmental stress on lithium-ion batteries in electrochemical energy storage systems [J]. Chinese Journal of Power Sources, 2025,49(09):1813-1823. (in Chinese).

[5] Wang X J. Research and design of a linear Li-ion battery charge management chip. Xidian University, 2023. (in Chinese).

[6] Rahul, K., Meena, R. K., Gupta, R. K., Iyer, P. K., Tej, M. A., & Nath, S. (2018, October). Battery charging of smart phones using organic solar cells. In 2018 2nd IEEE International Conference on Power Electronics, Intelligent Control and Energy Systems (ICPEICES) (pp. 1-5). IEEE.

[7] Ahmad, R. W., Gani, A., Hamid, S. H. A., Shojafar, M., Ahmed, A. I. A., Madani, S. A., ... & Rodrigues, J. J. (2017). A survey on energy estimation and power modeling schemes for smartphone applications. International Journal of Communication Systems, 30(11), e3234.

[8] Lu, M. H. M., Hack, M., Hewitt, R., Weaver, M. S., & Brown, J. J. (2008). Power consumption and temperature increase in large area active-matrix OLED displays. Journal of display technology, 4(1), 47-53.

[9] Lo'ai, A. T., Basalamah, A., Mehmood, R., & Tawalbeh, H. (2016). Greener and smarter phones for future cities: Characterizing the impact of GPS signal strength on power consumption. IEEE access, 4, 858-868.

[10] Rumi, M. A., & Hasan, D. H. (2015, September). CPU power consumption reduction in android smartphone. In 2015 3rd International Conference on Green Energy and Technology (ICGET) (pp. 1-6). IEEE.

[11] Kucinskis G, Bozorgchenani M, Feinauer M, et al. Arrhenius plots for Li-ion battery ageing as a function of temperature, C-rate, and ageing state: an experimental study [J]. J Power Sources, 2022, 549: 232129.

[12] Yu Q H, Li Y H, Sun G X, et al. Double-layer optimal configuration of wind storage microgrid capacity and economy considering temperature and battery life [J]. Science Technology and Engineering, 2025,25(25):10726-10734. (in Chinese)

[13] Huang, J., Li, J., & Li, Z. (2021). A state of health rapid assessment method for decommissioned lithium-ion batteries. Power Syst. Prot. Control, 49, 25-32. (in Chinese)

[14] Lv, S., Wang, X., Lu, W., Zhang, J., & Ni, H. (2021). The influence of temperature on the capacity of lithium ion batteries with different anodes. Energies, 15(1), 60.

[15] Ait Saadi, H., Ykhlef, F., & Guessoum, A. (2011, March). MCMC for parameters estimation by Bayesian approach. In Eighth International Multi-Conference on Systems, Signals & Devices (pp. 1-6). IEEE.

[16] Couderc, N., Reichenbach, C., & Söderberg, E. (2023, May). Performance Analysis with Bayesian Inference. In *2023* IEEE/ACM 45th International Conference on Software Engineering: New Ideas and Emerging Results (ICSE-NIER) (pp. 112-116). IEEE.

[17] Egidio, L. N., Hansson, A., & Wahlberg, B. (2021, July). Learning the step-size policy for the limited-memory Broyden-Fletcher-Goldfarb-Shanno algorithm. In 2021 International Joint Conference on Neural Networks (IJCNN) (pp. 1-8). IEEE.

[18] Immer, A., Korzepa, M., & Bauer, M. (2021, March). Improving predictions of Bayesian neural nets via local linearization. In International conference on artificial intelligence and statistics (pp. 703-711). PMLR.

[19] Juda Lithium Battery. Cold weather drains phone batteries quickly! Why are lithium-ion batteries so afraid of the cold? https://m.juda.cn/news/236284.html

[20] Pan, J., Zheng, Y., Ning, L., & Ding, Q. (2012, October). A New Viewpoint on Chaotic Signal in Communication: Viewing from Random Variables and Random Process. In 2012 Fifth International Workshop on Chaos-fractals Theories and Applications (pp. 176-180). IEEE.

[21] Deen, M. J., & Marinov, O. (2005, August). Noise in advanced electronic devices and circuits. In AIP Conference proceedings (Vol. 780, No. 1, pp. 3-12). American Institute of Physics.

[22] Chen, X., Nixon, K. W., & Chen, Y. (2016, September). Practical power consumption analysis with current smartphones. In 2016 29th IEEE International System-on-Chip Conference (SOCC) (pp. 333-337). IEEE.

[23] Chen, C., Zhang, K. Z., & Zhao, S. J. (2015, April). Examining the effects of perceived enjoyment and habit on smartphone addiction: The role of user type. In International Conference on E-Technologies (pp. 224-235). Cham: Springer International Publishing.

[24] Karmore, S. P., Mahajan, A. R., & Kitey, S. (2013, September). Battery monitoring and analysis for android based system. In 2013 15th International Conference on Advanced Computing Technologies (ICACT) (pp. 1-6). IEEE.

[25] Daud, S., Ahmad, R. B., Lynn, O. B., Abd Kareem, Z. I., Kamarudin, L. M., Ehkan, P., ... & Othman, R. R. (2014, August). The effects of CPU load & idle state on embedded processor energy usage. In 2014 2nd International Conference on Electronic Design (ICED) (pp. 30-35). IEEE.

Funding

This research received no external funding.

Conflicts of Interest

The authors declare no conflict of interest.

Acknowledgment

This paper is an output of the science project.

Open Access